Electronic Supplemental Information

Synergistic single process additive manufacturing of hydro-responsive Ag nanoparticle composites by digital visible light processing 3D printing

[1]Sokhna I. Y. Diouf, [1]Darrick J. Williams, [1]Alejandra Londoño-Calderon, [1]Michael T. Pettes, [2]Sönke Seifert, and [1,3]Millicent A. Firestone*

[1]Materials Physics & Applications Division, Los Alamos National Laboratory, Los Alamos, NM USA 87545
[2] X-ray Sciences Division, Argonne National Laboratory, Lemont, IL USA 60439
[3]Lawrence Berkeley National Laboratory, Berkeley, CA USA 94720

(*) Author to whom correspondence should be addressed:
Millicent A. Firestone
Lawrence Berkeley National Laboratory
One Cyclotron Rd
M/S 50R4049
Berkeley, CA 94720
Phone: 510-220-3946
E-mail: mafirestone@lbl.gov

Experimental

Materials and Methods. PEO_{75}-PPO_{30}-PEO_{75} (Pluronic F68) was received from BASF Corporation (Mount Olive, NJ). Lyophilized dimyristoyl-sn-glycero-3-phosphocholine (DMPC) was purchased from Avanti Polar Lipids (Alabaster, AL). Lauryldimethylamine-N-oxide (LDAO) was purchased from Calbiochem-Novabiochem Corp. (LaJolla, CA). Poly(ethylene glycol) diacrylate (PEGDA, M_n 700), triethanolamine (TEOA), eosin Y, and silver nitrate (99.0%) were purchased from Sigma-Aldrich (Milwaukee, WI). All reagents were reagent grade or better and used as received. Absolute ethanol (KOPTEC, King of Prussia, PA) was used as received. Milli-Q (18 MΩ cm^{-1}) water was used where applicable.

F68 diacrylate. The nonionic triblock copolymer, PEO_{75}-PPO_{30}-PEO_{75}, F68 was used as received and acrylated as previously described.[15] F68 (2.0 g,0.24 mmol) was dissolved in anhydrous dichloromethane (60 mL) at room temperature followed by addition of K_2CO_3 (1.0 g, 7.2 mmol). Distilled acryloyl chloride (0.39 ml, 0.7 mmol) was added dropwise over a 2-5 min timeframe. The reaction mixture was stirred for 12 h at room temperature. Potassium carbonate was removed from the reaction mixture by filtration through Cellite™ (Ward Hill, MA) supported on a glass frit. The $F68(Acr)_2$ solution was reduced under vacuum at 35°C to yield a viscous liquid. The product was precipitated with Et_2O (60 mL), filtered, and dried under vacuum to remove the volatile impurities. The extent of polymer functionalization was determined by ^1H NMR spectroscopy as previously described.[14] Functionalization ranges were determined to be between 80-95 %.

Preparation of $F68(Acr)_2$-based complex fluid. A typical mixture consisted of Φ_L = 0.0672 ± 0.005 DMPC lipid (Fig. 1 (1)), Φ_P= 0.147 ± 0.003 $F68(Acr)_2$ (Fig. 1 (2)), Φ_S = 0.0371 ± 0.0003 LDAO co-surfactant (Fig. 1 (3)), Φ_{PEGDA} = 0.00595 ± 0.0005 PEGDA M_n 700 (Fig. 1 (4)), Φ_i = 0.0118 ± 0.0002 eosin y (Fig. 1 (5)), Φ_{base}= 0.00445 ± 0.00004 TEOA (Fig. 1 (6)) in Φ_w = 0.746 ± 0.001 water. Hydration of the DMPC, $F68(Acr)_2$, and LDAO was first carried out by repeated cycles of heating (50°C) and vortex mixing until a macroscopically optically uniform sample was obtained. Next, the crosslinking co-macro-monomer, PEGDA, base, TEOA, and visible light photo-initiator (eosin Y) was added and vortex mixed until a homogeneous mixture is achieved. The complex fluid mixture is centrifuged briefly to eliminate bubbles introduced through mixing. Typically, Ag NP composites are prepared by addition of 24 μL of a 1.04 M $AgNO_3$ aqueous solution to the complex fluid mixture to yield a final concentration of 9.34 mM Ag^+. Variations in Ag^+ concentrations were evaluated as noted in the text. Complex fluids should be tightly capped (to prevent water evaporation) and wrapped in Al foil (to inhibit ambient light-initiated reduction of Ag^+ and polymerization).

Vat-photopolymerization. DLP 3D printing was performed on a Kudo3D Titan 2 (Dublin, CA). The printer employs a digital light projector as the illumination source (λ > 395 nm). Printing using the manufacturer pre-calibrated settings gave a resolution of ~ 50 μm. Creation Workshops suite was used to slice .stl files generated using CAD software (Solidworks) or files downloaded from open sources. A custom-made circular build plate (2.5 cm diameter, 6 mm height) was machined with drilled out holes (2 mm diameter holes). The build plate was painted black to minimize light reflection into the complex fluid resin. Undesirable air bubbles during complex fluid loading were manually eliminated prior to initiating 3D printing. Optimized Printing parameters included; the layer thickness, L (0.5 mm to 2 mm), light exposure time, Δt_{print} (25- 90 s), lift speed, ΔS_{lift} (10 – 20 mm s^{-1}), submersion speed, ΔS_{down} (10- 25 mm s^{-1}), and dwell time, Δt_{dwell} (0.3 - 0.5 s). Parameters, ΔS_{lift}, ΔS_{down}, Δt_{dwell} were selected based upon starting recommendations from the DLP 3D printer manufacturer. The optimized parameters provided a balance between resolution (L), degree of polymerization (Δt_{print}), and adherence to the build platform (Δt_{print}). Dwell time was adjusted to allow the resin a chance to equilibrate before the next layer was printed. L > 100 μm was possible but printing objects with finer features was limited as a result. Δt_{print} < 20 seconds gave incomplete polymerization and the builds lacked sufficient mechanical strength to be self-supporting. ΔS_{lift} > 5 mm s^{-1} caused the build to partially separate from the platform and/or remain adhered to the polymerization vat. Changes to the resin formulation (PEGDA concentration or eosin Y/TEOA visible light photo-initiating catalyst system, etc.) will require re-optimization of some parameters. Builds were removed from the build platform using a razor blade. Gross surface excess resin was removed with a Chemwipe, followed by rinsing in DI water. Extent of polymerization was monitored by ATR/FT-IR spectroscopy. Completeness of Ag(I) reduction was probed by UV-Vis optical spectroscopy on water swollen builds to monitor time-dependent

loss of both Ag(I) or loosely bound Ag(0). Oxidation of the *in-situ* synthesized Ag NPs in the hydrogels is minimized in the absence of a strong oxidizer such as peroxide.[1]

The depth of the light source penetration, D_L, due to the Ag NPs can be estimated using an established relationship.[2] The relationship states that D_L is inversely related to the extinction coefficient of the absorber, ε_A, and the concentration of the absorber, [A]. Here, for ~ 10 mM [Ag^+] and ~ 20 nm Ag NP (with an extinction coefficient[3] of 4.2 x 109 $Lmol^{-1}cm^{-1}$, [3] a D_L of ~ 0.25 μm is estimated. A benefit of the current resin formulation is the ability to readily alter Ag^+ concentration over a wide range, and/or to adjust NP size, thereby allowing for either increasing or decreasing the D_L as needed.

[1] L. E. Valenti, C. E. Giacomelli,. J Nanopart. Res. 2017, 19, 156-165
[2] S. C. Ligon, R. Liske, J. Stampfl, M. Gurr, R. Mulhopf, Chem. Rev. 2017, 117, 10212-10290
[3] D. Paramelle, A Sadovoy, S. Gorelik, P Free, J. Hobley, D. G. Fernig Analyst, 2014, 139, 4855-4861.

Physical Methods. ATR / FT-IR spectroscopy was performed using a Thermo Scientific spectrometer over the wavenumber range 4000 - 400 cm^{-1} with spectra recorded at 4 cm^{-1} resolution and averaged over 256 scans. Thermogravimetric analysis (TGA) was carried out on a TA Instrument Q500 by heating a known amount of sample (1-5 mg) in a platinum pan from 20 °C, to a final temperature of 500 °C, at a rate of 5 °C/min under N_2 flow. Dynamic mechanical analysis (DMA) was performed using a TA Instrument Q800 on samples printed with dimensions of 14.4 mm × 5.4 mm × 1.7 mm (l x h x w). Data were collected in tension mode with constant oscillation at 1 Hz from 30 °C to 70 °C at a rate of 3 °C min^{-1} under Ar flow (100 mL min^{-1}). The maximum amplitude was 5 μm, the dynamic force and static force were 3.98 N and 0.02 N, respectively. UV/Visible spectroscopy was collected using a Shimadzu UV2600 spectrophotometer (Kyoto, Japan) operating in single beam configuration over the wavelength region 200 - 900 nm. Temperature control was achieved using a Peltier element (Shimadzu TCC-100 Thermoelectrically Controlled Cell holder) inserted in the spectrophotometer. Diffuse reflectance measurements were made using a DT-1000 CD UV-Vis light source equipped with a SD2000 charge-coupled device (CCD) under OOI Base 32 software (Ocean Optics, Dunedin, FL).

Transmission Electron Microscope (TEM) analysis was carried out on released NPs dropwise deposited on ultra-thin carbon TEM grids. Briefly, the well-entrained NPs can only be released from the polymer matrix by disrupting the crosslinks through treatment with an aqueous solution of hydrazine. Typically, less than 100 mg Ag NP polymer composite is swollen in 2 mL of water for 2 h, followed by the addition of 1 mL of a 37 (V/V) % aqueous solution of hydrazine. After ca. a day, the solid material dissolved, leaving an orange-brown colored solution. These samples were imaged using an image corrected FEI Titan 80-300 kV microscope at the LANL Electron Microscopy Laboratory operating at 80 kV. High-angle annular dark field S/TEM (HAADF-STEM) images of the composite were collected at 80 kV using a camera length of 100 mm and a C2 aperture of 70 μm.

Small- and wide-angle X-ray scattering (SWAXS) measurements were performed using the pin-hole setups at the undulator beamline 12ID at the Advanced Photon Source (APS) at Argonne National Laboratory (Lemont, IL). Data collected at station C (12/18 keV) used either a custom-built CCD detector composed of 4 CCD chips featuring a 180 mm square active area with 1024 × 1024 pixels resolution or a MARCCD detector composed of 9 CCD chips featuring 300 mm square active area with 2048 × 2048 pixels resolution. The sample-to-detector distance provided a *q*-range from 0.006 – 0.6 $Å^{-1}$ or 0.005 – 0.7 $Å^{-1}$. Data collected at station B simultaneously collected both SAXS and WAXS data using both a Pilatus 2M detector for SAXS and a Pilatus 300K for WAXS. For all measurements, the scattering vector, *q*, was calibrated with silver behenate employing the characteristic diffraction ring at q = 0.1076 $Å^{-1}$. The collected scattering images were averaged to produce plots of scattered X-ray intensity, I(q), versus the scattering vector, q, where $q = 4\pi \sin(\theta)/\lambda$. Durable, self-supporting polymers were supported on a custom-built holder. The averaged scattering patterns were background subtracted using data collected on air.

Fig. S1. (A) Dynamic mechanical analysis (DMA) of 3D printed Ag NP hydrogel (crosslinked, de-swollen, prepared with 2.33 mM $AgNO_3$) composites (at 1.00 Hz). The storage modulus (E') and tan δ range from 228 MPa at 27°C to 0.65 MPa at 70°C (black) and 0.1 at 30 °C to 0.3 at 70 °C (red), respectively. (B) DMA of 3D printed hydrogel (crosslinked, de-swollen) lacking Ag NPs at 1.00 Hz. The storage modulus (E') and tan δ range from 69 MPa at 27°C to 0.49 MPa at 60°C (black) and 0.1 at 30 °C to 0.32 at 60 °C (red), respectively. (C) DMA profiles collected by varying Ag^+ concentration. The observed changes in the storage modulus and tan δ for the Ag NP hydrogel composite is a competition between detrimental filler-polymer (hydrogel) interactions (i.e., physical or chemical attachments) and reinforcement derived from a filler percolated (fractal) network. Thus, the slightly diminished Tan δ for the composite *vs.* the hydrogel possibly reflects increased stiffness upon filler production.

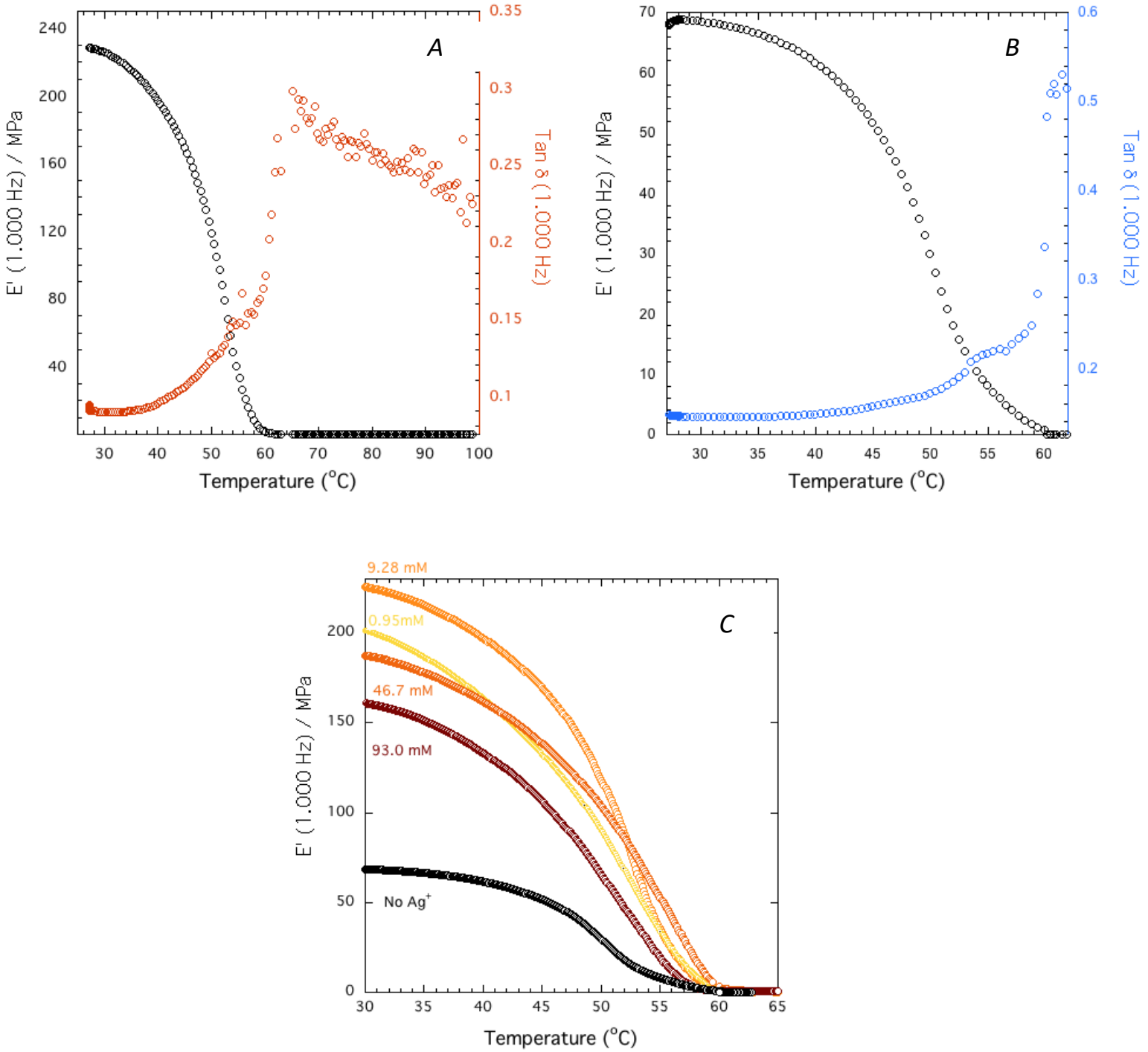

Fig. S2. Drawings used for DLP printing a flower of life (A) and honeycomb (B). The size of the prints derived from the .stl files are shown in the figure below (white) and compared to that experimental recorded immediately post printing (orange), and after fully swollen (24 h) in water (blue). Ag hydrogel composite printed with 9.34 mM $AgNO_3$.

A.

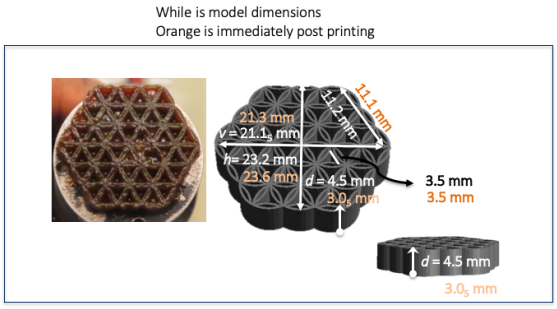

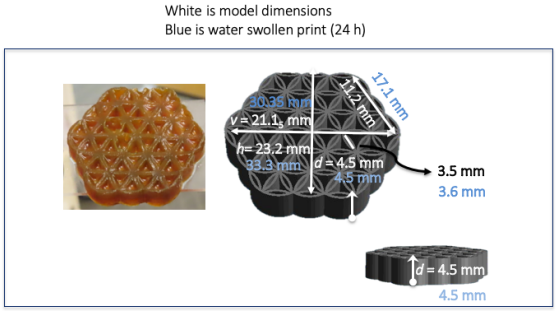

B.

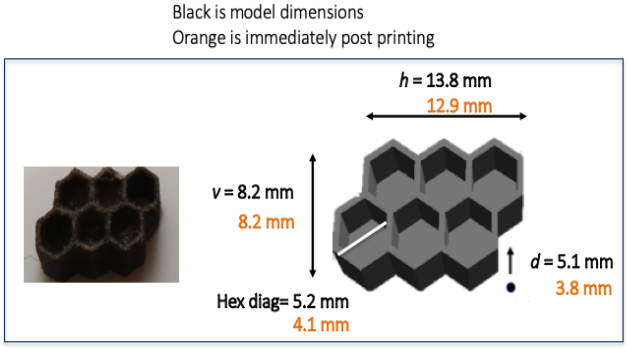

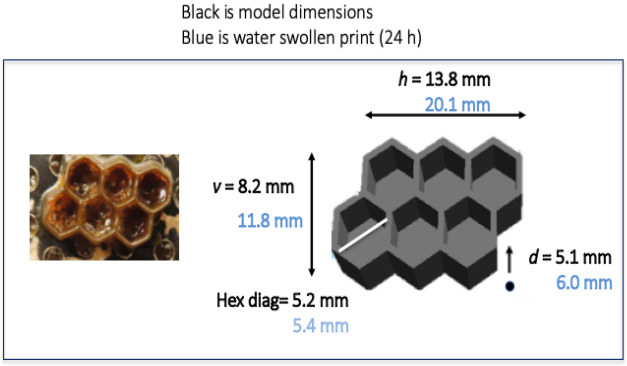

Fig. S3. Drawings used for DLP printing a flower of life (A) and honeycomb (B). The size of the prints derived from the .stl files are shown in the figure below (white) and compared to that experimental recorded immediately post printing (orange), and after fully swollen (24 h) in water (blue). No $AgNO_3$ introduced into the mesophase prior to printing.

A.

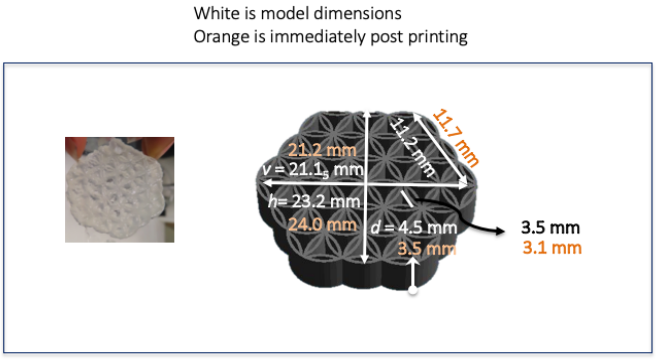

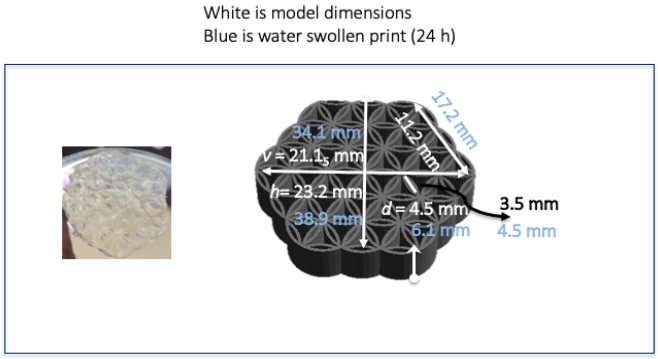

B.

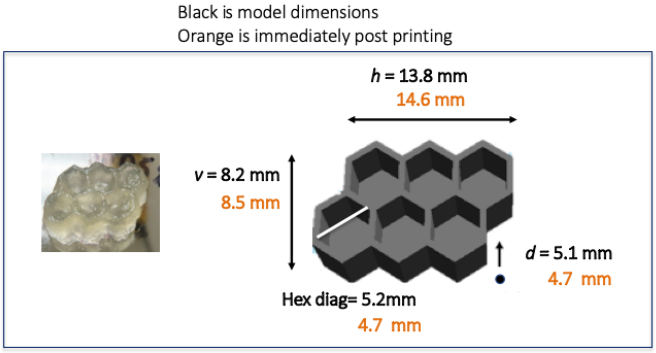

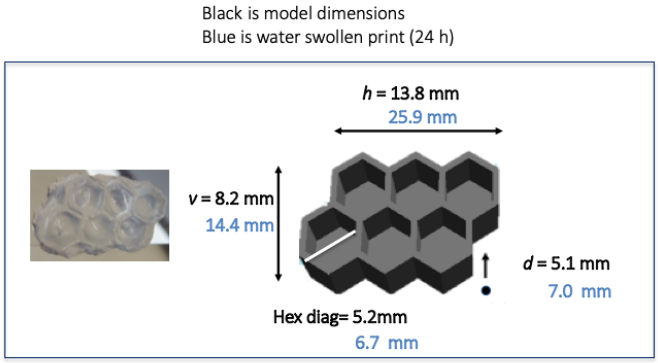

Fig. S4. ATR/FT-IR spectrum recorded on the Ag NP polymer hydrogel composite. Successful acrylation is corroborated through the absence of the acrylate signature mode at 1725 cm^{-1} (C=O stretching) in conjunction with the appearance of a strong vibrational mode at 1738 cm^{-1}, signaling production of unconjugated acryloyl carbonyls. A weak mode at 1763 cm^{-1} is also found consistent with the presence of saturated ester groups. Collectively, the modes confirm the acrylate moieties at the ends of the $F68(Acr)_2$ macromonomer and PEGDA have crosslinked into a polymer network.

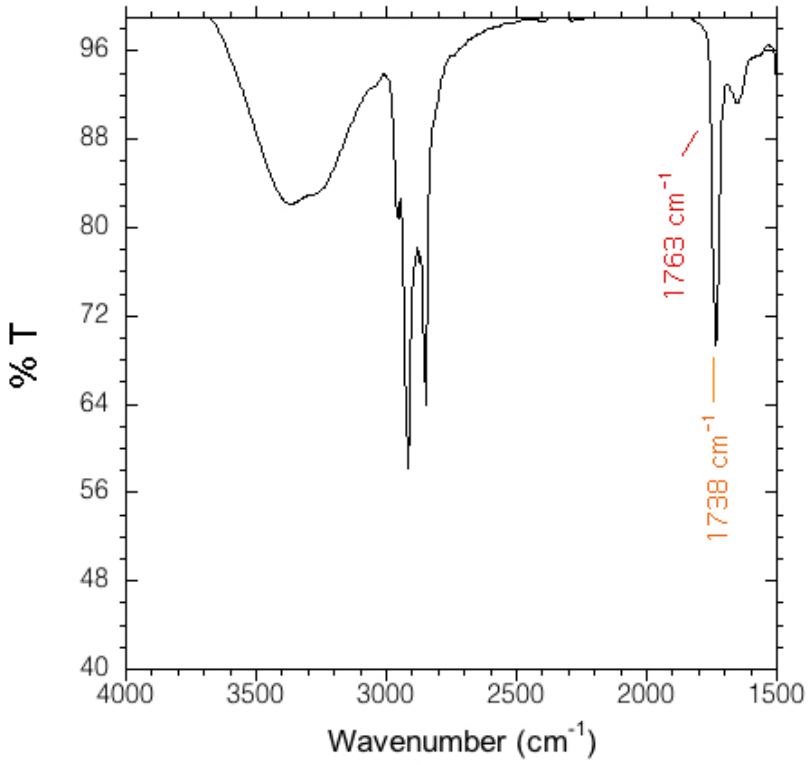

Fig. S5. SAXS of 3D printed hydrogel lacking Ag NPs

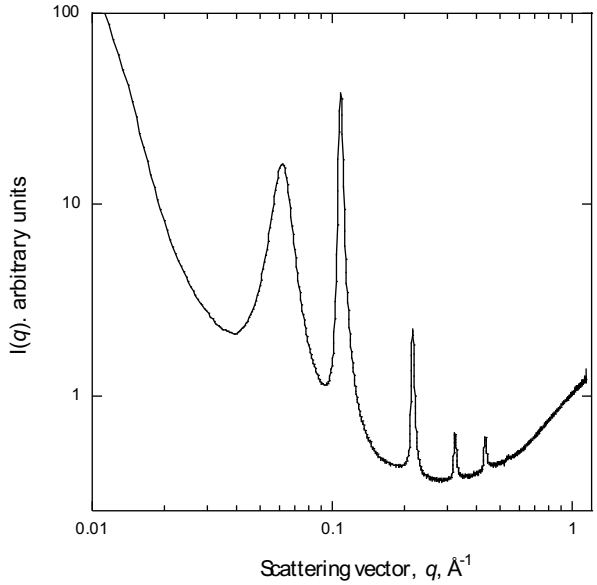

Fig. S6. (A)TGA collected on a Ag NP hydrogel composite. Measurement made (A) immediately after printing. (B) fully dehydrated